

Unexpected charge effects strengthen pi-stacking pancake bonding

Zhong-hua Cui,^{1,5*} Meng-hui Wang,¹ Hans Lischka,^{3,4} Miklos Kertesz^{2*}

¹ *Institute of Atomic and Molecular Physics, Key Laboratory of Physics and Technology for Advanced Batteries (Ministry of Education), Jilin University, Changchun, 130012, PR China*

² *Chemistry Department and Institute of Soft Matter, Georgetown University, Washington, D.C. 20057-1227*

³ *Department of Chemistry and Biochemistry, Texas Tech University, Lubbock, TX, 79409*

⁴ *A School of Pharmaceutical Science and Technology, Tianjin University, 300072 Tianjin, PR China*

⁵ *Beijing National Laboratory for Molecular Sciences, 100190 Beijing, PR China*

*Corresponding Authors: zcui@jlu.edu.cn; kertesz@georgetown.edu

Abstract

Phenalenyls (PLYs) are important synthons in many functional and electronic materials which often display favorable molecule to molecule overlap for electron or hole transport. They also serve as a prototype for π -stacking pancake bonding based on two electron multicenter bonding (2e/mc). Unexpected near doubling of binding energy is obtained for the positively charged PLY_2^+ dimer with a similar effect seen for the positively charged olympicenyl (OPY) radical dimer. This charge effect is reversed for the perfluorinated (PF) dimers and the negatively charged perfluorinated (PF) dimers, PF- PLY_2^- and PF-OPY $_2^-$ become strongly bound. Long range interactions reflect these differences. Also surprising is that in this case the pancake bonding corresponds to single electron (1e/mc) or a three electron (3e/mc) multicenter bonding in contrast to 2e/mc bonding that occurs for the neutral radical dimers. The strong preference for large intermolecular overlap is maintained in these charged dimers. Importantly, the preference for π -bonding compared to σ -bonding is strongly enhanced as compared to the neutral PLY dimers.

Keywords: Pancake bond, Intermolecular interactions, pi-stacking, fluorinated phenalenyl dimer, charged pi-dimers, MR-AQCC theory.

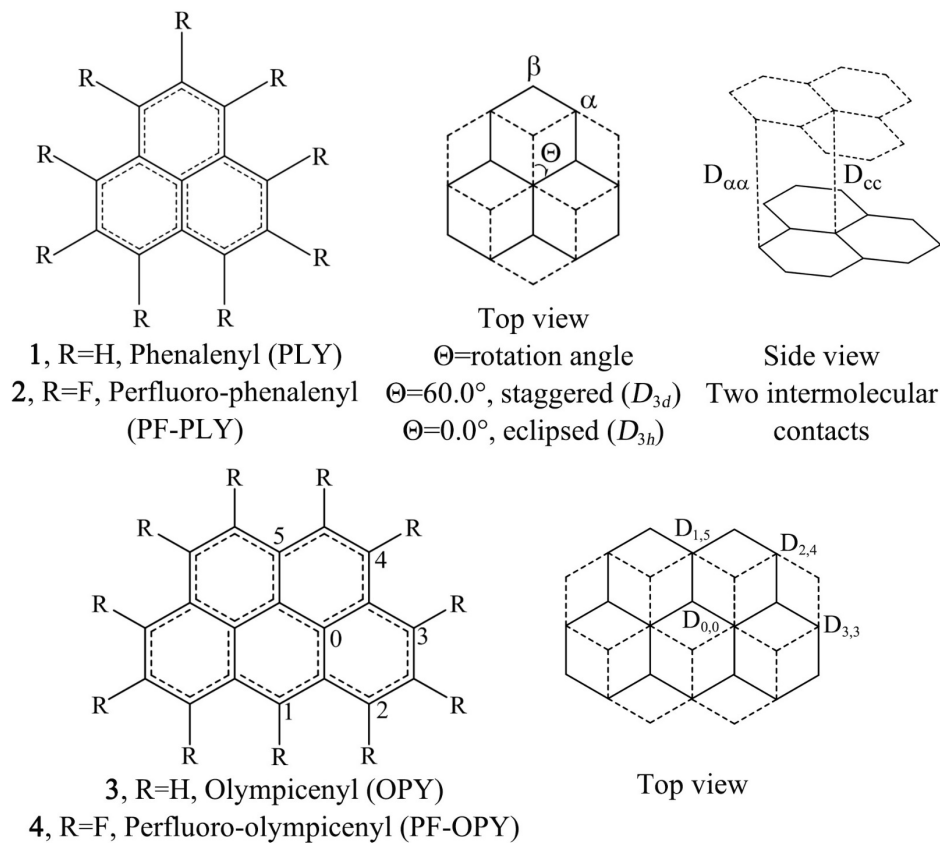
1. Introduction

π -stacking configurations are ubiquitous in aggregates of polycyclic aromatic hydrocarbons (PAHs) and other conjugated molecules often driven by ordinary non-covalent van der Waals interactions. A quite unconventional mechanism occurs when multicenter partially covalent electron sharing between conjugated radicals leads to π -stacking often resulting in highly conducting organic crystals.¹⁻⁵ In addition to its importance in conducting organics, this type of intermolecular interaction is increasingly recognized as a driving force of aggregation among π -conjugated neutral and charged (ionic) radicals.⁶⁻⁹ Many molecules in this category have exciting optoelectronic and magnetic properties and their potential to exploit unpaired spin densities of the monomers to engineer exceptionally close π – π contacts.¹⁰⁻¹¹

This effect has been referred to as “pimerization” or “pancake bonding”¹²⁻²¹ and it occurs when the overlap between the two singly occupied π -molecular orbitals (SOMOs) undergo spin-pairing creating diamagnetic dimers and larger aggregates. Recent progress both in the experiments and computational modeling have shown that this mechanism is robust and sufficiently wide spread. Key features of these unique intermolecular interactions include shorter than van der Waals (vdW) contacts²² and directional atom-over-atom packing geometries in contrast to atom over bond or atom over ring packing typical of closed shell molecules.^{12, 14} For many applications a critical question is to avoid σ -bond formation so that the highly overlapping π -stacking configuration can be maintained. We shall see momentarily that in addition to the avoidance of σ -bond formation with bulky side groups²⁰ an alternative mechanism is offered by partial charging.

Hitherto unexplained aspect of pancake bonding is the high prevalence of partly charged pancake bonded dimers, trimers, and other aggregates. Should pancake bonding be strongly affected by introducing charge into a pancake bonded dimer? In their pioneering study, Small et al.¹⁵ compared the dimerization energy of the neutral and +1 charged dimers of the prototypical pancake bonding molecule, phenalenyl (PLY, **1**). They found through wave

function quantum chemistry at the CP-MRMP2/6-31G(d) level that the PLY_2^+ cation radical dimer is bound by 20 kcal/mol vs the neutral dimer is bound by only 11 kcal/mol. Given the fact that the former has a formal pancake bond order (PBO, see equ. 1) of only $\frac{1}{2}$ vs. 1 for the latter, they found that while the covalent contribution is reduced and the dispersion interactions remained largely unchanged, the difference is mainly due to an increase of electrostatic attraction.²³ We are expanding these findings by comparing cationic and anionic dimers of PLY and olympicenyl (OPY, 2), and their perfluorinated derivatives which are illustrated in Scheme 1.²⁴ The problem is important because the number of charged pancake bonded systems is much larger than the neutral ones,^{8-9, 25-28} see e.g. these recent examples.²⁹⁻³²



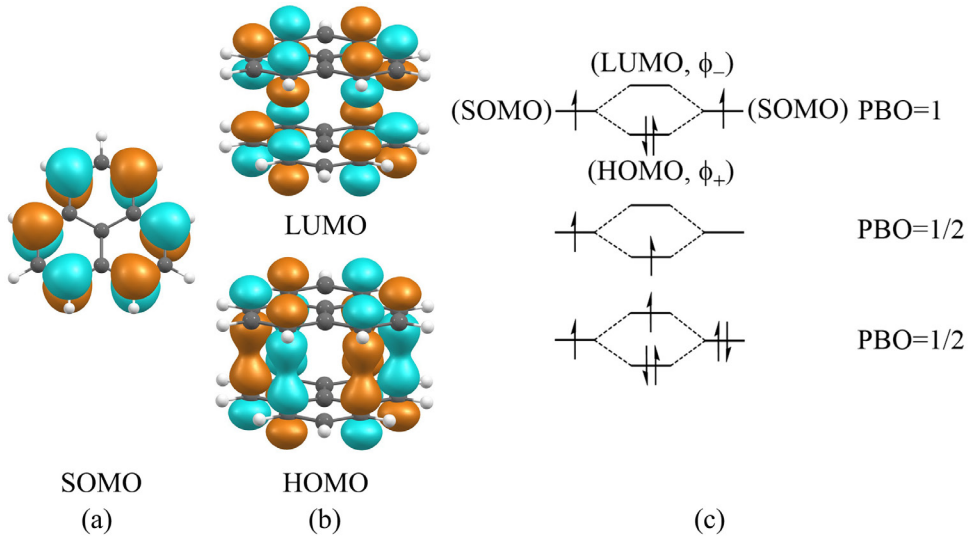
Scheme 1. Monomers, dimer complexes and their key parameters studied in this work. Notice the atom over atom stacking in the dimers indicative of some covalent character in intermolecular bonding interaction. The PLY_2 dimer displays a two electron 12 center (2e/12c) bonding at the D_{3d} symmetry, the $(\text{OPY})_2$ dimer²¹ displays a two electron 20 center

(2e/20c) bonding at the C_{2h} symmetry. See also Scheme S2.

Scheme 2 illustrates for PLY and its neutral and charged dimers a molecular orbital interaction diagram for three types of pancake bonding under discussion here: two-electron multicenter bonding (2e/mc) with $PBO = 1$, one electron multicenter bonding (1e/mc) with $PBO = \frac{1}{2}$, and three electron multicenter bonding (3e/mc) also with $PBO = \frac{1}{2}$. Here PBO stands for a formal through space pancake bond order defined as:¹⁵

$$PBO = \frac{1}{2}(N_{\text{bind}} - N_{\text{anti}}) \quad (1)$$

where N_{bind} is the number of electrons in the bonding orbitals and N_{anti} is the number of electrons in antibonding orbitals. As a practical matter, only the intermolecular bonding and antibonding orbitals need to be counted.



Scheme 2. (a) Singly occupied molecular orbital of the PLY radical localized on α -carbons. Scheme S1 illustrates the SOMO for OPY. (b) Bonding and antibonding combination of the two SOMOs in a pancake bonding configuration with D_{3d} π -stacking geometry. (c) Formal pancake bond orders (PBOs) of a neutral radical dimer, a dimer cation and a dimer anion.

The main components of the interactions between the two phenalenyls in each dimer are analyzed using dissociation and rotational potential energy surface (PES) scans. Rotational scans are particularly insightful for PLY dimers because the SOMO-SOMO overlap can be turned on (D_{3d} , $\theta = 60^\circ$) or turned off ($\theta = 30^\circ$). Such a simple tool is not available for OPY due to its lower symmetry. Partly for this reason, we also engage an energy

decomposition analysis (EDA)³³⁻³⁴ that is applicable regardless of symmetry. We rely to a large extent on the high-level multireference averaged coupled cluster (MR-AQCC/6-31G(d))³⁵ method which has shown good performance³⁶⁻³⁷ due to the balance for the description of multireference effects (static electron correlation) induced by the two near lying orbitals, φ_+ and φ_- , illustrated in Scheme 2, and dynamic electron correlation responsible for the dispersion-type intermolecular electron correlation energy. Additionally, appropriate DFT computations have been performed.

2. Computational Methods

The geometries of the neutral phenalenyl (PLY, **1**) and olympicenyl (OPY, **3**), and additionally perfluoro-phenalenyl (PF-PLY, **2**) and perfluoro-olympicenyl (PF-OPY, **4**) dimers and their singly charged cationic and anionic analogues were optimized using the (U)M05-2X/6-311G(d) level of theory,³⁸ in which the broken-symmetry spin unrestricted (U) formalism was used for the neutral species. All isomers were confirmed as local minima using frequency computations. The geometries of all neutral and singly charged dimers considered here were also fully optimized by MR-AQCC/3-21G for the neutral, +1 and -1 charged dimers of both PLY and PF-PLY. Additionally, the geometries of the neutral, +1 and -1 charged dimers of PLY were also optimized with MR-AQCC using the larger 6-31G(d) basis. Good agreement between the results obtained with the two basis sets was found, which was used as justification of continuing the MR-AQCC calculations with the computationally much more efficient smaller basis set. Molecular orbitals (MOs) created by the CASSCF method were used in the MR-AQCC calculations with the same CAS(2,2) as used in the CASSCF calculations for the neutral ones,³⁹ whereas the state-averaged (SA) CAS(1,2) and CAS(3,2) calculations were used for the optimization of the cationic and anionic species, respectively. MR-AQCC/3-21G was used to compute the rigid rotation and dissociation potential energy scans for all the neutral and charged dimers. The MR-AQCC calculations were performed using the COLUMBUS program suite.⁴⁰⁻⁴¹ The unpaired electron population analysis⁴²⁻⁴³ was computed using the TheoDORE program.⁴⁴⁻

45

For interpretative purposes the separation of the different energy terms is highly desirable, especially the separation of the covalent-like bonding interaction due to the SOMO-SOMO overlap producing the electron delocalization over the dimer vs. the vdW interaction, E_{vdW} .

E_{vdW} includes dispersion, Pauli (steric) repulsion and electrostatic interactions. We found it useful to separate the vdW component (E_{vdW}), from the attractive SOMO-SOMO interaction, ($E_{SOMO-SOMO}$), a term reflecting a covalent-like component of the interaction energy.^{39, 46} This decomposition, albeit approximate, is useful for two reasons. First, there are no directly applicable energy decompositions schemes available for the MR-AQCC method while the presented energy decomposition, shown below, is applicable for it as well as for any other approach including DFT. This scheme is based on total energies computed with the respective method and does not rely on any asymptotic expansion scheme of the interaction energy. Second, this decomposition provides essential insights by allowing to focus on the SOMO-SOMO interaction component which is driving the pancake bonding interaction.^{39, 46}

The following procedure is applied for the neutral pancake bonded dimers.^{39, 46}

$$E_{int}(R) = E_{Total}(R) - E_{Total}(\text{at } 10.0 \text{ \AA}) = -E_{binding}, \quad (2)$$

where R stands for the contact distance between the monomers. The key assumption is that the two components of the interaction are approximately additive:

$$E_{int} = E_{SOMO-SOMO} + E_{vdW} \quad (3)$$

The E_{vdW} term is approximated by the interaction energy of the high spin state (triplet in this case), E_{int}^T taken at the same unrelaxed ground state geometry of the singlet.⁴⁶

$$E_{vdW} \approx E_{int}^T \text{ (at the geometry of the singlet)} \quad (4)$$

The interaction energy and its components at the equilibrium geometry of the singlet are particularly relevant and will be listed and discussed. These assumptions were justified and validated for PLY₂.³⁸⁻³⁹

The following approximation will be used for both the neutral and the charged PLY and PF-PLY dimers:

$$E_{\text{SOMO-SOMO}}(60^\circ) \approx E_{\text{int}}(60^\circ) - E_{\text{int}}(30^\circ) \quad (5)$$

An important aspect of this approximation is that it is applicable for the singly charged PLY_2 and PF-PLY_2 dimers, while the approximation based on equations (3) and (4) is not applicable because these are doublet ground state dimers. As a validation we refer to reference 38, where the rotation based method and the multiplicity based method gave very close estimates for the value of $E_{\text{SOMO-SOMO}}$.

The intermolecular Coulomb interaction energy (E_{Coul}) is defined by equ (6),

$$E_{\text{Coul}} = \sum \frac{q_i * q_j}{d_{ij}} \quad (6)$$

where the q_i and q_j are the atomic charges and d_{ij} are the distances between the atoms i and j. Summation is limited to atom pairs that belong to different monomers in the dimer.

We also used as an alternative the energy decomposition analysis (EDA) developed by Ziegler and Rauk³⁴ using (U)PBE0-MBD⁴⁷/TZP level of theory with the ADF⁴⁸ program package. The many body dispersion (MBD) refers to the method of Tkatchenko et al.⁴⁷ that provides an accurate description of vdW interactions that includes both screening effects and a high order treatment of the many-body van der Waals energy. The interaction energy and its components are denoted here differently from equations (3)-(4) or (5) with a Δ to refer specifically to the EDA analysis. ΔE_{int} is the difference between the energy of the dimer and the energies of the constituent monomers. In the current case it is divided into four main components as follows.

$$\Delta E_{\text{int}} = \Delta E_{\text{elstat}} + \Delta E_{\text{Pauli}} + \Delta E_{\text{orb}} + \Delta E_{\text{disp}} \quad (7)$$

The term ΔE_{elstat} corresponds to the quasi-classical electrostatic interaction between the unperturbed charge distributions calculated from the orbital densities. The Pauli repulsion, ΔE_{Pauli} , contains the destabilizing interactions between electrons of the same spin on either fragment. The orbital interaction ΔE_{orb} accounts for charge transfer, delocalization and polarization effects. The vdW interaction energy in this scheme, ΔE_{vdW} , is then approximately the sum of the dispersion interaction, electrostatic interaction and Pauli repulsion:

$$\Delta E_{\text{vdW}} = \Delta E_{\text{disp}} + \Delta E_{\text{elstat}} + \Delta E_{\text{Pauli}} \quad (8)$$

Further computational details are summarized in the Supporting Information (SI), Section 2.

3. Results and Discussion

We present results in four subsections. First, we show strong evidence that in contrast to pancake bonding with PBO=1, where σ -bonded configurations are often energetically competitive with π -stacking configurations,⁴⁹ this is not the case with PBO=1/2 dimers.⁵⁰ Then, evidence is provided that π -stacking geometries are maintained for PBO=1/2 dimers showing subtle but systematic differences between positively and negatively charged dimers in correlation with the presence or absence of perfluorination. This is then put into the context of the total energy computations showing that, surprisingly, while the perfluorinated anion dimers have stronger pancake bonding with PBO=1/2, for the parent unflourinated ones it is the cations with the stronger pancake bonding. Interpretation, including energy component analysis, indicates that changes in the intermolecular electrostatics plays a key role in this effect.¹⁵

The stability of the π -dimer vs. σ -dimer

σ -bonded configurations are often energetically competitive with π -stacking configurations as shown for example by the presence of fluxional bonding in some phenalenyls^{49,51} and their derivatives.⁵² Therefore, we first investigate the effect of fluorine substitution and the total charge on the relative energies of the dimers of PLY and OPY, with key data summarized in Table 1; the structures are illustrated in Figure S2. We obtained consistent results with previous work⁴⁹⁻⁵⁰ for neutral PLY₂. For neutral PLY₂ amongst the five σ - and one π -dimer configurations the π -dimer is slightly less stable than the σ -dimer while the σ -dimer is more stable by 7.8 kcal/mol for neutral PF-PLY₂. The relative stability is reversed for each of the charged species with the π -stacking configuration becoming more stable. Note that σ -bonding in a phenalenyl dimer is relatively weak compared to ordinary CC σ -bonds, due to the reduced π -conjugation and the stress induced by pyramidalization in a planar framework.⁴⁹⁻⁵⁰

Table 1. Relative energies in kcal/mol of π and σ dimers of neutral and charged PLY₂ (**1₂**) and PF-PLY₂ (**2₂**) at the UM05-2X/6-311G(d) level.

	π^a	σ^b (RR1)	σ^b (RR2)	σ^b (RR3)	σ^b (RS1)	σ^b (RS2)
1₂	0.0	-2.6	-2.9	-4.1	-1.2	-4.0
2₂	0.0	-7.8	-7.1	-7.9	-6.4	-7.1
	π^a	$\pi(1)^c$	$\pi(2)^c$	$\pi(3)^c$	$\pi(4)^c$	$\pi(5)^c$
1₂	0.0	8.4	5.7	6.3	- ^d	8.3
1₂⁻	0.0	3.2	3.4	4.6	4.4	3.2
1₂⁺	0.0	10.3	7.0	9.3	11.0	8.5
2₂	0.0	8.5	5.1	5.5	- ^d	7.4
2₂⁻	0.0	12.4	8.3	9.5	12.6	10.7
2₂⁺	0.0	3.0	3.2	5.8	5.7	3.0

^a π -stacking dimer, D_{3d}. ^bNotation for σ -dimer configurations are from ref⁵⁰ and are illustrated in Figure S2. ^cThe lower symmetry π -stacked structures are illustrated in Figure S3. ^dConverges to $\pi(3)$, for details, see Tables S5 and S6.

The corresponding charged species present a totally different picture. Since these species have a formal PBO = 1/2, one expects the σ -bonds to be much weaker since only one unpaired electron is available. Indeed, during the geometry optimization process aiming to obtain σ -dimers, we started from the optimized geometries of the various neutral σ -dimers, but all these optimizations converged to various π -dimers with novel unique structures each displaying local minima with only one or two close contacts between α -carbon atoms. Most importantly, we were unable to find during geometry optimization any local minima corresponding to a σ -dimer. Note, that all these additionally identified π dimers (listed in Table 1 and illustrated in Figure S3) are less stable and in most cases significantly less stable than the staggered D_{3d} π -dimer configuration. This indicates that the multicenter pancake bonding even with one electron (1e/mc) shows strong preference for the maximum of the SOMO-SOMO overlapping geometry. We will gain further insights into this effect based on the geometry and energy analysis in the next sections.

The relative weakness of the σ -bonded configuration for the singly charged PLY₂ can be understood as follows. First, the σ -bond is much weaker for a single electron bond vs. a two-electron bond. Second, the local pyramidalization needed for σ -bond formation

distorts the rigid plane of the π -conjugated monomer and disrupts the conjugation also disfavoring the σ -dimer compared to the π -dimer configuration. Third, shorter intermolecular distances in the σ -dimer increase the Coulomb repulsion compared to the π -dimer. These effects make the π -dimer configuration more favorable compared to the σ -dimer so much so that σ -dimers do not even exist as local minima for the charged PLY₂ and PF-PLY₂ dimers. It appears that many pancake-bonded molecular dimers and larger aggregates avoid σ -bonding due to these effects.^{31-32, 53-54}

The effect of charge on the structures of the π -dimers

The most remarkable charge effect can be seen in comparing the direct C-C intermolecular distances in the geometries of the optimized twelve π -dimers, four neutral ones with full PBO=1, and eight charged ones with PBO=1/2 given in Table 2 and Table S7. Note that the geometry optimization at the MR-AQCC/6-31G(d) level for the PLY systems shown in Table S7 displays the same trends as the DFT geometry data shown in Table 2. The surprising overall observation is that all of these contact distances without exception are significantly shorter than 3.40 Å, the vdW distance for C...C contacts. Due to its SOMO orbital, both PLY⁺ and PLY⁻ are stable making the preparation of these charged dimer species viable. The cationic PLY₂⁺ has clearly shorter average intermolecular distances as compared to the anionic species, PLY₂⁻, while both correspond to PBO = 1/2. The situation is reversed for the perfluorinated species where PF-PLY₂⁺ has significantly longer intermolecular distances as compared to the anionic species, PF-PLY₂⁻. Similar trends are seen in the charged dimers of OPY and PF-OPY. This is quite significant, because it implies a control over contact distances, and thereby allowing a control of bandwidths in pancake bonded systems not seen before.

Table 2. Intermolecular carbon-carbon distances in Å of the neutral and charged PLY (**1**), PF-PLY (**2**), OPY (**3**), and PF-OPY (**4**) π -stacking pancake bonded dimers. All geometries refer to optimized structures by (U)M05-2X/6-311G(d). All neutral and charged dimers of **1** and **2** have D_{3d} symmetry, all neutral and charged dimers of **3** and **4** have C_{2h} symmetry. Atomic numbering corresponds to Scheme 1.

	Bond order, PBO	D _{cc} (D _{0,0})	D _{αα} (D _{3,3})	D _{2,4}	D _{1,5}	Average ^c
1₂	1	3.061	2.991	—	—	3.001
1₂⁺	½	3.187	3.191	—	—	3.190
1₂⁻	½	3.248	3.210	—	—	3.215
2₂	1	3.099	2.981	—	—	2.998
2₂⁺	½	3.166	3.052	—	—	3.068
2₂⁻	½	3.120	3.016	—	—	3.031
3₂	1	3.186	3.148	3.175	3.161	3.169
3₂⁺	½	3.202	3.246	3.234	3.188	3.221
3₂⁻	½	3.274	3.233	3.245	3.250	3.249
4₂	1	3.164	3.015	3.049	3.097	3.075
4₂⁺	½	3.185	3.052	3.069	3.118	3.099
4₂⁻	½	3.171	3.028	3.059	3.107	3.085
1₂ (Exp. ^a)	1	3.109 (3.201)	3.176 (3.306)	—	—	3.188 (3.291)
3₂ (Exp. ^b)	1	3.216 (3.257)	3.203 (3.256)	3.205/3.210 (3.180/3.327)	3.182 (3.225)	3.200 (3.247)

Exp. indicates the inclusion of bulky side groups in the computation and the respective experimental value is in parenthesis. ^aref 20. ^bref 21. ^cAverage direct C_α...C_α contact distances.

Energetics of the π-dimers

The interaction energy values are collected in Table 3 for all twelve dimeric species discussed in this work. Table S9 provides validation results at a higher optimization level for the six smaller system.

Table 3. Intermolecular interaction energies and their Esomo-Somo components of the neutral and charged PLY (**1**), PF-PLY (**2**), OPY (**3**), and PF-OPY (**4**) dimers obtained by MR-AQCC/6-31G(d)//UM05-2X/6-311G(d).

	1₂	1₂⁺	1₂⁻	2₂	2₂⁺	2₂⁻
E _{int}	-10.8	-19.6	-11.3	-16.7	-16.9	-25.7
Esomo-Somo	-22.3	-15.1	-12.0	-13.9	-13.3	-11.7
E _{vdW}	11.5	-4.5	0.7	-2.8	-3.6	-14.0
	3₂	3₂⁺	3₂⁻	4₂	4₂⁺	4₂⁻
E _{int}	-10.9	-21.8	-12.9	-15.7	-20.0	-28.3
Esomo-Somo	-14.1	— ^a	— ^a	-10.3	— ^a	— ^a
E _{vdW}	3.1	— ^a	— ^a	-5.4	— ^a	— ^a

^aData not available, see text below equ. (5).

The most prominent result is that the largest binding energy (most negative interaction energy) is obtained not for the dimers with $\text{PBO} = 1$, but for specific charged dimers with the bond order of only $\text{PBO} = \frac{1}{2}$. This unusual effect was first observed for $\mathbf{1}_2^+$ and was attributed to electrostatic effects.⁵⁰ Here we find that the effect extends to $\mathbf{3}_2^+$, as well as $\mathbf{2}_2^-$ and $\mathbf{4}_2^-$. This complex behavior, especially the dependency on the sign of the charge on the dimer, needs interpretation: the binding energy is larger for positively charged dimers of PLY and OPY, and larger for the negatively charged dimers of the perfluorinated species, PF-PLY and PF-OPY. The differences are dramatic considering the scale of typical intermolecular interactions adding approximately 9~13 kcal/mol to the binding energy according to Table 2 for $\mathbf{1}_2^+$, $\mathbf{2}_2^-$, $\mathbf{3}_2^+$, and $\mathbf{4}_2^-$ compared to their neutral counterparts. In what follows we trace the enhancement of the interaction to electrostatic effects.

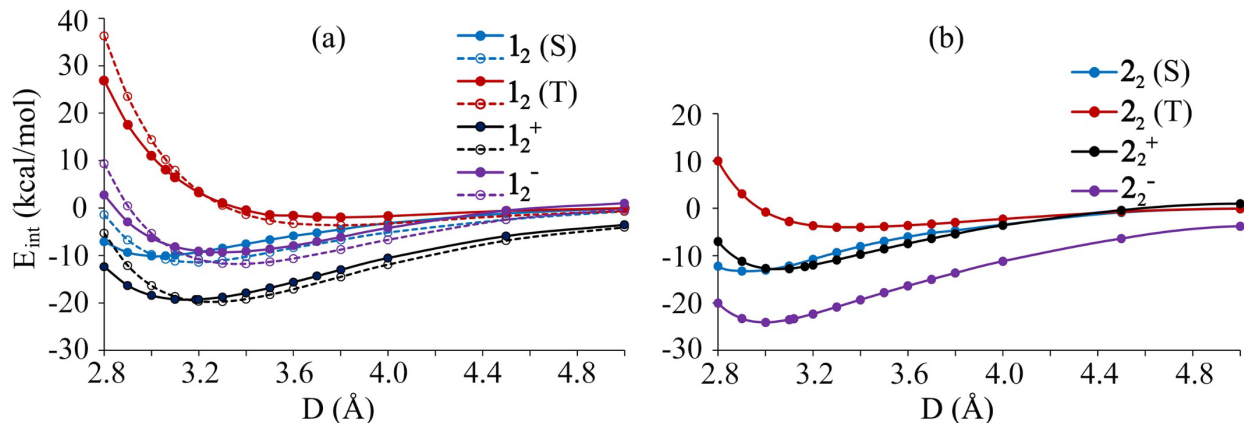


Figure 1. Rigid dissociation energy scans of singlet and triplet states of the phenalenyl dimer ($\mathbf{1}_2$, PLY₂) and of the doublet states of the charged phenalenyl dimers (PLY₂⁺ and PLY₂⁻) in the D_{3d} staggered configuration as a function of the intermolecular distance (D_{cc}) using MR-AQCC(n,2)/3-21G, where the n=1, 2, 3 correspond to the cationic, neutral and anionic dimers, respectively. The scans of the neutral and the charged PF-PLY dimers ($\mathbf{2}_2$) are shown in (b). In (a), dashed line corresponds to the MR-AQCC(n, 2)/6-31G(d) level.

The total energy scans provide further insights. Figure 1 shows energy scans with respect to the intermolecular distance, D_{cc} for the all six PLY dimers plus the triple of the two neutral ones. Note, that the 3-21G basis set presents a good performance with reference to the 6-31G(d) (Figure 1a, dashed line) using the MR-AQCC method. The significant electrostatic interaction accounts for the lowest E_{int} in the cationic PLY_2^+ and anionic $PF-PLY_2^-$ dimers to be discussed in the next subsection.

Most striking is the fact that even at long range, where overlap is nearly negligible, clearly enhanced interaction appears for PLY_2^+ compared to both PLY_2 and PLY_2^- , while for the perfluoro case the opposite charge is preferred: $PF-PLY_2^-$ is more stable near dissociation compared to $PF-PLY_2$ and PLY_2^+ . This behavior provides another strong evidence that the preference is directed by the electrostatic interaction in the distance range relevant for pancake bonding. At distances shorter than the equilibrium distances for the dimers, the orders of some of these states interchange as shown in Figure 1.

Next, we analyze the interaction energy by reporting rotational scans based on the M05-2X/6-311G(d) geometries and using energy at the MR-AQCC/6-31G(d) level. The respective E_{vdW} and $E_{SOMO-SOMO}$ terms for all six PLY-based dimers are listed in Table 3. While the approximations presented in equations (3) and (4) do not separate out the electrostatic component from the dispersion attraction and Pauli repulsion components, we can discuss the rest of the trends as follows. For PLY_2 the total vdW term is positive, and it contains some Pauli repulsion due to the shorter than vdW contacts. The negative charge distributed in the intermolecular space in the neutral dimer provides another repulsive term. The latter is reduced in the positively charged PLY_2^+ compared to the negatively charged PLY_2^- . The elongated CC contacts in the charged dimers mentioned in connection with Table 2 reduces the Pauli repulsion. Assuming that changes in the dispersion energy are less sensitive to the single charge added to the dimer, this explains that the total vdW interaction turns into a negative (attractive) value for PLY_2^+ and become less repulsive for PLY_2^- as compared to the neutral PLY_2 dimer. For the $PF-PLY_2$ series, the effects of the signs of charges are reversed, as discussed above.

For the PLY_2 dimer, the $E_{SOMO-SOMO}$ term is significantly reduced in the charged species as compared to the neutral one, but the vdW repulsion that includes the reduced

electrostatic repulsion even becomes attractive in the cationic dimer. Thus, the largest binding energy occurs for the cationic dimer despite the reduced $E_{\text{SOMO-SOMO}}$. The $E_{\text{SOMO-SOMO}}$ terms all are smaller in the PF-PLY₂ series as compared to the PLY₂ series, but the vdW interaction becomes attractive for PF-PLY₂⁺, especially, the anionic PF-PLY₂⁻ dimer has a large attractive vdW interaction, leading to the largest binding energy in the perfluorinated series. The reduction of the SOMO-SOMO interaction in the PLY₂ series upon charging affects the overall properties of pancake bonded systems, because this reduction amounts to a reduction of the strong preference for specific orientations for pancake bonded systems. Nevertheless, as demonstrated by the data in Figure S1(c) and Table 3, the SOMO-SOMO energy term leads to a barrier of 12 to 22 kcal/mol between the low and high energy conformers, a sufficiently large driving force to strongly favor one of the two atom-over-atom configurations, which in the case of all PLY dimers discussed, is the D_{3d} staggered configuration.

Consequences of the electrostatic environment

In this subsection we trace the following trends based on the computed total interaction energies shown in Table 3 to differences in intermolecular electrostatic interactions in the dimers under study.

These trends are:

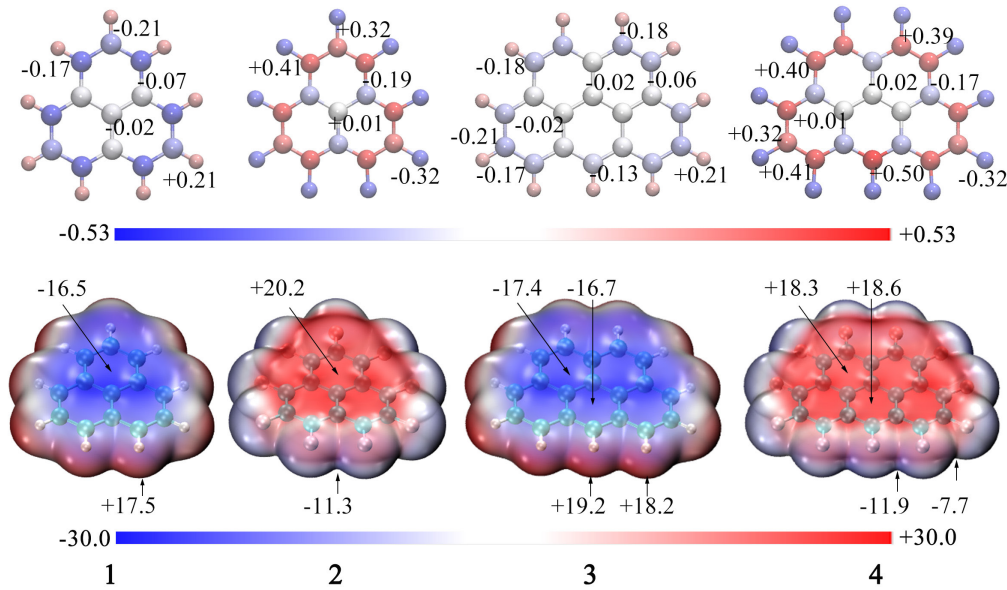
1. For the unflourinated dimers the absolute values of the interaction energies are larger by 8-9 kcal/mol for the positively charged dimers: **1₂**⁺vs. **1₂**⁻, and **3₂**⁺, **3₂**⁻.
2. For the perfluorinated dimers the absolute values of the interaction energies are larger by 8-9 kcal/mol for the negatively charged dimers: **2₂**⁻ vs. **2₂**⁺, and **4₂**⁻ vs. **4₂**⁺.

The same trends are reflected in the average optimized contact distances (in Table 1) that are slightly shorter for the *positively* charged unflourinated dimers, and slightly shorter for the *negatively* charged perfluorinated dimers, respectively.

We employ qualitative arguments, followed by two approaches to energy decomposition: Coulomb interaction energies based on the atomic point charge model and a Morokuma-Ziegler-Rauk-type EDA.^{33-34, 55-56} It is worth mentioning that energy decomposition is

capable only to provide trends, since the interaction energy component terms are not physical observables.⁵⁷

These trends in the CC contact distances can be qualitatively understood on the basis of the charge distributions around the monomers as illustrated in Scheme 3 which highlights that the charge distributions and electrostatic potentials have the opposite sign between unflourinated and perfluorinated monomers. The strongly polarized distribution of the atomic charges in PLY^- and PF-PLY^+ is at the source of their relatively longer contacts compared to the oppositely charged PLY^+ and PF-PLY^- , respectively. Based on the charge distribution in Scheme 3 and Scheme S2 (charged species), the efficient way to reduce the intermolecular electrostatic repulsion would require extra positive charge for PLY and OPY , and extra negative charge on PF-PLY and PF-OPY .



Scheme 3. NPA charge distribution in $|e|$ (top row) and electrostatic potential (ESP) (bottom row) in kcal/mol mapped on the van der Waals surface ($\rho=0.001$ a.u. isosurface) of the neutral unsubstituted PLY (**1**) and OPY (**3**) and perfluoro-substituted PF-PLY (**2**) and PF-OPY (**4**) computed by UM05-2X/6-311G(d).

We follow up these arguments with Coulomb interaction energies based on point charges summarized in Tables 4 and S8(a)-(b). Atomic charges, as is well known, can differ strongly.

But the atomic point charge based intermolecular Coulomb interaction is well defined by equ. (6).

Table 4. Intermolecular Coulomb interaction energy (E_{Coul}) in kcal/mol of dimers based on atomic point charges from Natural Population Analysis (NPA) by UM05-2X/6-311G(d). All geometries correspond to the optimized structures except for the triplet that corresponds to the geometry of the optimized singlet.

	1₂^a	1₂⁺	1₂⁻	1₂^b
E_{Coul}	15.9	19.2	42.4	15.6
	2₂^a	2₂⁺	2₂⁻	2₂^b
E_{Coul}	31.8	63.8	31.0	31.8
	3₂^a	3₂⁺	3₂⁻	3₂^b
E_{Coul}	18.1	19.7	45.0	17.9
	4₂^a	4₂⁺	4₂⁻	4₂^b
E_{Coul}	35.9	67.3	34.0	35.9

^aSinglet. ^bTriplet.

These data support the qualitative conclusions based on the charge distributions of the monomers discussed above in connection with Scheme 3. The singlet and triplet Coulomb interaction energy terms of the neutral dimers are virtually the same for all four systems in line with equ. (4). More importantly, comparing the positively charged non-fluorinated **1₂⁺** and **3₂⁺** to the negatively charged **1₂⁻** and **3₂⁻**, the latter are strongly destabilized by approximately 23 to 25 kcal/mol. This substantial effect is the source of the relative preference of the positively charged dimers vs. the negatively charged dimers. For the perfluorinated dimers the charge preference has the opposite sign: here the negatively charged dimers display an approximately 33 kcal/mol preference over the positively charged ones considering these point-charge based models for estimating the Coulomb repulsion. Due to their intrinsically arbitrary elements, these models are not conclusive, but they support the switch of preference between the positively and negatively charged dimers as a function of perfluorination.

The alternative to a point charge model for estimating intermolecular electrostatic interactions is to use quantum mechanical energy decomposition schemes. While such schemes are plagued by various limitations,⁵⁷⁻⁵⁸ still for the current purposes they provide useful insights into the origin of the charge effects under discussion. The respective data

are presented in Table 5 and Figure S4.

Table 5. Energy decomposition analysis (EDA, in kcal/mol) of the intermolecular interaction energy in the neutral and charged dimers of PLY (**1**), PF-PLY (**2**), OPY (**3**), and PF-OPY (**4**) using UPBE0-MBD/TZP//UM05-2X/6-311G(d) at the most stable D_{3d} and C_{2h} configurations. The terms refer to equ (7).

	1₂	1₂⁺	1₂⁻	2₂	2₂⁺	2₂⁻
ΔE_{int}	-12.9	-24.5	-15.6	-12.7	-18.2	-26.9
ΔE_{Pauli}	47.6	26.4	27.3	38.6	30.4	37.8
ΔE_{elstat}	-22.2	-16.2	-8.3	-15.2	-4.7	-23.0
ΔE_{disp}	-14.9	-12.6	-13.1	-18.3	-17.3	-18.1
ΔE_{orb}	-23.4	-22.2	-21.4	-17.8	-26.7	-23.7
	3₂	3₂⁺	3₂⁻	4₂	4₂⁺	4₂⁻
ΔE_{int}	-15.4	-28.3	-18.6	-18.0	-22.2	-30.7
ΔE_{Pauli}	40.8	35.0	34.0	44.7	40.8	45.7
ΔE_{elstat}	-19.2	-21.2	-11.9	-17.8	-9.0	-26.2
ΔE_{disp}	-20.7	-19.5	-20.0	-26.3	-25.6	-26.4
ΔE_{orb}	-16.3	-22.6	-20.7	-18.7	-28.4	-23.8

The key result of this analysis is as follows. The electrostatic energy, ΔE_{elstat} , provides a relative preference of -8 to -10 kcal/mol for **1₂⁺** and **3₂⁺** compared to **1₂⁻** and **3₂⁻** respectively. For the perfluorinated pairs this additional electrostatic stabilization is computed at -17 to -18 kcal/mol. While the specific decomposition depends on the details of the level of theory, and the overlap between the interacting molecules, there should be no doubt about the importance of the electrostatic component of the intermolecular interaction explaining the relative stabilities of these pancake bonded dimers as a function of charge *and* perfluorination.

A brief overview of the other terms of this EDA shows consistency with respect to the analysis based on equations (3) and (4). The orbital interaction term, ΔE_{orb} , accounts for the charge transfer, delocalization and polarization effects, which also can be considered as including the main contributions to the SOMO-SOMO interaction, while the other three

terms (ΔE_{elstat} , ΔE_{Pauli} and ΔE_{disp}) added together can be considered as representing the vdW interaction, E_{vdW} , as used in equ. (3) above. Figure S4 (a) and S4 (b) show the total energy curves of the four main components of the EDA as a function of θ for PLY₂ and PF-PLY₂, respectively. Figure S4 (c) displays the difference between singlet and triplet scans, which approximately represents the SOMO-SOMO interaction as per equations (3) and (4). Compared to the PLY₂ dimer, the SOMO-SOMO interaction is significantly reduced in the PF-PLY₂ dimer, fully consistent with our MR-AQCC analysis. Moreover, it reflects that the SOMO-SOMO interaction is the main component for the difference of the total interaction between singlet and triplet. On the other hand, ΔE_{elstat} and ΔE_{disp} are nearly constant, and the ΔE_{Pauli} has only small variations, indicating that E_{vdW} does not change significantly from 60° to 30° again consistent with our MR-AQCC analysis.

For the neutral dimers in their singlet states, the orbital term is smaller in PF-PLY₂ as compared to PLY₂, but the former has a larger dispersion term, which is consistent with the rotational scans. Comparing the different charged PLY₂ or PF-PLY₂ dimers, the electrostatic term is a crucial factor to strengthen the interaction as reflected in ΔE_{int} . This provides further evidence that the PLY₂⁺ and PF-PLY₂⁻ have stronger overall pancake bonds compared to the oppositely charged dimers, PLY₂⁻ and PF-PLY₂⁺, respectively.

Additional supporting evidence for this interpretation is provided by data in Table S10, which displays the total number of effectively unpaired electrons for all 12 dimers under discussion. This parameter signals a degree of electron unpairing on a comparable scale across each of the two series. These data confirm the trends showing that electron pairing is reduced (N_U increased) upon charging dimers moving from $\text{PBO} = 1$ to $1/2$ as expected, further underlining the point that the strengthening of pancake bonding upon this charge effect is not due to increased electron pairing but to a reduced electrostatic repulsion between the PAHs.

4. Conclusion

As a practical matter, properly charged pancake bonded systems can increase their stability and avoid σ -bonding more easily compared to neutral pancake bonding.

The second observation is that the charged dimers can display stronger pancake bonding compared to the neutral radical based dimers even though charging reduces the formal pancake bond order from 1 to $\frac{1}{2}$. The associated intermolecular distances with PBO = $\frac{1}{2}$ are typically longer than those of pancake bonds with PBO = 1.

The interaction energy in charged pancake bonded systems is less dominated by the SOMO-SOMO interactions, and electrostatic effects become more important. The reduced SOMO-SOMO interaction in the PLY₂ and OPY₂ series upon charging is still sufficiently robust to maintain their strong preferences for specific orientations typical for pancake bonded systems by maintaining maximum overlap with atom-over-atom configurations.

Conflict of Interest

There is no conflict of interest to report.

Acknowledgements

This work was funded by the National Natural Science Foundation of China (No. 11874178, 11922405, 91961204). This work was supported by Beijing National Laboratory for Molecular Sciences (BNLMS201910). MK is member of the Georgetown University Institute of Soft Matter. Computer time was partially provided by the School of Pharmaceutical Science and Technology, Tianjin University on the computer cluster Arran, which is gratefully acknowledged.

Supporting information

Atomic notation; SOMO coefficients; computational details; energy scans; structures and coordinates of dimers; energy decomposition; Coulomb energies; charge distribution; physical properties.

References

1. Schafer, D. E.; Wudl, F.; Thomas, G. A.; Ferraris, J. P.; Cowan, D. O.; Apparent Giant Conductivity Peaks in an Anisotropic Medium: TTF-TCNQ. *Solid. State. Commun.* **1974**, 14, 347–351.
2. Soos, Z. G.; Klein, D. J.; in Molecular Association. in Molecular Association, Academic, New York, **1975**, Vol. 1 (Ed.: R. Foster).

3. Heeger, A. J.; in *Highly Conducting One-Dimensional Solids*. in *Highly Conducting One-Dimensional Solids*, Springer, Boston, **1979**, Pp. 69–145.

4. Miller, J. S.; *Extended Linear Chain Compounds* [Vols 1–3]. **1982**.

5. Pal, S. K.; Itkis, M. E.; Tham, F. S.; Reed, R. W.; Oakley, R. T.; Haddon, R. C.; Resonating valence-bond ground state in a phenalenyl-based neutral radical conductor. *Science* **2005**, 309, 281–284.

6. Chen, P. C.; Metz, J. N.; Mennito, A. S.; Merchant, S.; Smith, S. E.; Siskin, M.; Rucker, S. P.; Dankworth, D. C.; Kushnerick, J. D.; Yao, N.; Zhang, Y. L.; Petroleum pitch: Exploring a 50-year structure puzzle with real-space molecular imaging. *Carbon* **2020**, 161, 456–465.

7. Geraskina, M. R.; Dutton, A. S.; Juetten, M. J.; Wood, S. A.; Winter, A. H.; The Viologen Cation Radical Pimer: A Case of Dispersion-Driven Bonding. *Angew. Chem., Int. Edit.* **2017**, 56, 9435–9439.

8. Penneau, J. F.; Stallman, B. J.; Kasai, P. H.; Miller, L. L.; An Imide Anion Radical That Dimerizes and Assembles into. Pi.-Stacks in Solution. *Chem. Mater.* **1991**, 3, 791–796.

9. Kosower, E. M.; Cotter, J. L.; Stable Free Radicals. II. The Reduction of 1-Methyl-4-cyanopyridinium Ion to Methylviologen Cation Radical. *J. Am. Chem. Soc.* **1964**, 86, 5524–5527.

10. Tian, Y. H.; Kertesz, M.; Is There a Lower Limit to the CC Bonding Distances in Neutral Radical pi-Dimers? The Case of Phenalenyl Derivatives. *J. Am. Chem. Soc.* **2010**, 132, 10648–10649.

11. Haddon, R. C.; Design of Organic Metals and Superconductors. *Nature* **1975**, 256, 394–396.

12. Kertesz, M.; Pancake Bonding: An Unusual Pi-Stacking Interaction. *Chem. -Eur. J.* **2019**, 25, 400–416.

13. Preuss, K. E.; Metal-radical coordination complexes of thiazyl and selenazyl ligands. *Coordin. Chem. Rev.* **2015**, 289, 49–61.

14. Devic, T.; Yuan, M.; Adams, J.; Fredrickson, D. C.; Lee, S.; Venkataraman, D.; The maximin principle of pi-radical packings. *J. Am. Chem. Soc.* **2005**, 127, 14616–14627.

15. Small, D.; Zaitsev, V.; Jung, Y. S.; Rosokha, S. V.; Head-Gordon, M.; Kochi, J. K.; Intermolecular, pi-to-pi bonding between stacked aromatic dyads. Experimental and theoretical binding energies and near-IR optical transitions for phenalenyl radical/radical versus radical/cation dimerizations. *J. Am. Chem. Soc.* **2004**, 126, 13850–13858.

16. Jung, Y. S.; Head-Gordon, M.; What is the nature of the long bond in the TCNE_2^{2-} pi-dimer? *Phys. Chem. Chem. Phys.* **2004**, 6, 2008–2011.

17. Lu, J. M.; Rosokha, S. V.; Kochi, J. K.; Stable (long-bonded) dimers via the quantitative self-association of different cationic, anionic, and uncharged pi-radicals: Structures, energetics, and optical transitions. *J. Am. Chem. Soc.* **2003**, 125, 12161–12171.

18. Jakowski, J.; Simons, J.; Analysis of the electronic structure and bonding stability of the TCNE dimer dianion $(\text{TCNE})_2^{2-}$. *J. Am. Chem. Soc.* **2003**, 125, 16089–16096.

19. Novoa, J. J.; Lafuente, P.; Del Sesto, R. E.; Miller, J. S.; Exceptionally long (≥ 2.9 angstrom) C-C bonds between $[\text{TCNE}]^-$ ions: Two-electron, four-center $\pi^* \cdot \pi^*$ C-C bonding in $\pi\text{-}[\text{TCNE}]_2^{2-}$. *Angew. Chem., Int. Edit.* **2001**, 40, 2540–2545.

20. Goto, K.; Kubo, T.; Yamamoto, K.; Nakasuji, K.; Sato, K.; Shiomi, D.; Takui, T.; Kubota, M.; Kobayashi, T.; Yakusi, K.; Ouyang, J. Y.; A stable neutral hydrocarbon radical: Synthesis, crystal structure, and physical properties of 2,5,8-tri-tert-butyl-phenalenyl. *J.*

Am. Chem. Soc. **1999**, 121, 1619–1620.

21. Xiang, Q.; Guo, J.; Xu, J.; Ding, S. S.; Li, Z. Y.; Li, G. W.; Phan, O. A.; Gu, Y. W.; Dang, Y. F.; Xu, Z. Q.; Gong, Z. C.; Hu, W. P.; Zeng, Z. B.; Wu, J. S.; Sun, Z.; Stable Olympicenyl Radicals and Their pi-Dimers. *J. Am. Chem. Soc.* **2020**, 142, 11022–11031.
22. Miller, J. S.; Novoa, J. J.; Four-center carbon–carbon bonding. *Acc. Chem. Res.* **2007**, 40, 189–196.
23. Roach, A. C.; Baybutt, P.; Potential curves of alkali diatomic molecules and the origins of bonding anomalies. *Chem. Phys. Lett.* **1970**, 7, 7–10.
24. Hofmann, P. E.; Tripp, M. W.; Bischof, D.; Grell, Y.; Schiller, A. L. C.; Breuer, T.; Ivlev, S. I.; Witte, G.; Koert, U.; Unilaterally Fluorinated Acenes: Synthesis and Solid-State Properties. *Angew. Chem., Int. Edit.* **2020**, 59, 16501–16505.
25. Meot-Ner, M.; Dimer cations of polycyclic aromatics. Experimental bonding energies and resonance stabilization. *J. Phys. Chem.* **1980**, 84, 2724–2728.
26. Badger, B.; Brocklehurst, B.; Formation of Dimer Cations of Aromatic Hydrocarbons. *Nature* **1968**, 219, 263–263.
27. Howarth, O. W.; Fraenkel, G. K.; Electron Spin Resonance Study of Mono- and Dimeric Cations of Aromatic Hydrocarbons1. *J. Am. Chem. Soc.* **1966**, 88, 4514–4515.
28. Suzuki, S.; Morita, Y.; Fukui, K.; Sato, K.; Shiomi, D.; Takui, T.; Nakasuji, K.; Aromaticity on the pancake-bonded dimer of neutral phenalenyl radical as studied by MS and NMR spectroscopies and NICS analysis. *J. Am. Chem. Soc.* **2006**, 128, 2530–2531.
29. Bogdanov, N. E.; Milasinovi, V.; Zakharov, B. A.; Boldyreva, E. V.; Molcanov, K.; Pancake-bonding of semiquinone radicals under variable temperature and pressure conditions. *Acta. Crystallogr. B.* **2020**, 76, 285–291.

30. Starodub, T. N.; Cizmar, E.; Kliuikov, A.; Starodub, V. A.; Feher, A.; Kozlowska, M.; Stabilization of Pancake Bonding in $(\text{TCNQ})^2$ (center dot-) Dimers in the Radical-Anionic Salt $(\text{N-CH}_3\text{-2-NH}_2\text{-5Cl-Py})(\text{TCNQ})(\text{CH}_3\text{CN})$ Solvate and Antiferromagnetism Induction. *Chemistryopen*. **2019**, 8, 984–988.

31. Molcanov, K.; Jelsch, C.; Landeros, B.; Hernandez-Trujillo, J.; Wenger, E.; Stilinovic, V.; Kojic-Prodic, B.; Escudero-Adan, E. C.; Partially Covalent Two-Electron/Multicentric Bonding between Semiquinone Radicals. *Cryst. Growth. Des.* **2019**, 19, 391–402.

32. Molcanov, K.; Stalke, D.; Santic, A.; Demeshko, S.; Stilinovic, V.; Mou, Z. Y.; Kertesz, M.; Kojic-Prodic, B.; Probing semiconductivity in crystals of stable semiquinone radicals: organic salts of 5,6-dichloro-2,3-dicyanosemiquinone (DDQ) radical anions. *Crystengcomm*. **2018**, 20, 1862–1873.

33. Morokuma, K.; Why Do Molecules Interact? The Origin of Electron Donor-Acceptor Complexes, Hydrogen Bonding and Proton Affinity. *Acc. Chem. Res.* **1977**, 10, 294–300.

34. Ziegler, T.; Rauk, A.; On the Calculation of Bonding Energies by the Hartree Fock Slater Method. *Theor. Chim. Acta*. **1977**, 46, 1–10.

35. Szalay, P. G.; Bartlett, R. J.; Multi-Reference Averaged Quadratic Coupled-Cluster Method: A Size-Extensive Modification of Multi-Reference CI. *Chem. Phys. Lett.* **1993**, 214, 481–488.

36. Szalay, P. G.; Muller, T.; Gidofalvi, G.; Lischka, H.; Shepard, R.; Multiconfiguration Self-Consistent Field and Multireference Configuration Interaction Methods and Applications. *Chem. Rev.* **2012**, 112, 108–181.

37. Lischka, H.; Shepard, R.; Muller, T.; Szalay, P. G.; Pitzer, R. M.; Aquino, A. J. A.; do Nascimento, M. M. A.; Barbatti, M.; Belcher, L. T.; Blaudeau, J. P.; Borges, I.; Brozell, S.

R.; Carter, E. A.; Das, A.; Gidofalvi, G.; Gonzalez, L.; Hase, W. L.; Kedziora, G.; Kertesz, M.; Kossoski, F.; Machado, F. B. C.; Matsika, S.; do Monte, S. A.; Nachtigallova, D.; Nieman, R.; Oppel, M.; Parish, C. A.; Plasser, F.; Spada, R. F. K.; Stahlberg, E. A.; Ventura, E.; Yarkony, D. R.; Zhang, Z. Y.; The generality of the GUGA MRCI approach in COLUMBUS for treating complex quantum chemistry. *J. Chem. Phys.* **2020**, *152*, 134110.

38. Zhao, Y.; Schultz, N. E.; Truhlar, D. G.; Design of density functionals by combining the method of constraint satisfaction with parametrization for thermochemistry, thermochemical kinetics, and noncovalent interactions. *J. Chem. Theory. Comput.* **2006**, *2*, 364–382.

39. Cui, Z. H.; Lischka, H.; Beneberu, H. Z.; Kertesz, M.; Rotational Barrier in Phenalenyl Neutral Radical Dimer: Separating Pancake and van der Waals Interactions. *J. Am. Chem. Soc.* **2014**, *136*, 5539–5542.

40. Lischka, H.; Muller, T.; Szalay, P. G.; Shavitt, I.; Pitzer, R. M.; Shepard, R.; COLUMBUS-a program system for advanced multireference theory calculations. *Wires. Comput. Mol. Sci.* **2011**, *1*, 191–199.

41. Lischka, H.; Shepard, R.; Shavitt, I.; Pitzer, R. M.; Dallos, M.; Mueller, T.; Szalay, P. G.; Brown, F. B.; Ahlrichs, R.; Boehm, J. G.; Chang, A.; Comeau, D. C.; Gdanitz, R.; Dachsel, H.; Ehrhardt, C.; Ernzerhof, M.; Hoechtl, P.; Irle, S.; Kedziora, G.; Kovar, T.; Parasuk, V.; Pepper, M. J. M.; Scharf, P.; Schiffer, H.; Schindler, M.; Schueler, M.; Seth, M.; Stahlberg, E. A.; Zhao, J. G.; Yabushita, S.; Zhang, C. L.; Barbatti, M.; Matsika, S.; Schuurmann, M.; Yarkony, D. R.; Brozell, S. R.; Beck, E. V.; Blaudeau, J. P.; Ruckenbauer, M.; Sellner, B.; Plasser, F.; Szymczak, J. J.; COLUMBUS, an ab initio electronic structure program, release 7.0. **2017**.

42. Head-Gordon, M.; Characterizing unpaired electrons from the one-particle density matrix. *Chem. Phys. Lett.* **2003**, 372, 508–511.

43. Head-Gordon, M.; Reply to comment on 'characterizing unpaired electrons from the one-particle density matrix'. *Chem. Phys. Lett.* **2003**, 380, 488–489.

44. Plasser, F.; Bappler, S. A.; Wormit, M.; Dreuw, A.; New tools for the systematic analysis and visualization of electronic excitations. II. Applications. *J. Chem. Phys.* **2014**, 141, 024106.

45. Plasser, F.; TheoDORE: A Package for Theoretical Density, Orbital Relaxation, and Exciton Analysis, version 2.0. **2019**, <http://theodore-qc.sourceforge.net>.

46. Mota, F.; Miller, J. S.; Novoa, J. J.; Comparative Analysis of the Multicenter, Long Bond in [TCNE](center dot-) and Phenalenyl Radical Dimers: A Unified Description of Multicenter, Long Bonds. *J. Am. Chem. Soc.* **2009**, 131, 7699–7707.

47. Tkatchenko, A.; DiStasio, R. A.; Car, R.; Scheffler, M.; Accurate and Efficient Method for Many-Body van der Waals Interactions. *Phys. Rev. Lett.* **2012**, 108, 236402.

48. ADF 2020, SCM, Theoretical Chemistry, Vrije Universiteit, Amsterdam, The Netherlands, <Http://www.scm.com>.

49. Mou, Z.; Uchida, K.; Kubo, T.; Kertesz, M.; Evidence of sigma- and pi-Dimerization in a Series of Phenalenyls. *J. Am. Chem. Soc.* **2014**, 136, 18009–18022.

50. Small, D.; Rosokha, S. V.; Kochi, J. K.; Head-Gordon, M.; Characterizing the dimerizations of phenalenyl radicals by ab initio calculations and spectroscopy: sigma-bond formation versus resonance pi-stabilization. *J. Phys. Chem. A* **2005**, 109, 11261–11267.

51. Uchida, K.; Mou, Z. Y.; Kertesz, M.; Kubo, T.; Fluxional sigma-Bonds of the 2,5,8-

Trimethylphenalenyl Dimer: Direct Observation of the Sixfold sigma-Bond Shift via a pi-Dimer. *J. Am. Chem. Soc.* **2016**, 138, 4665–4672.

52. Morita, Y.; Suzuki, S.; Fukui, K.; Nakazawa, S.; Kitagawa, H.; Kishida, H.; Okamoto, H.; Naito, A.; Sekine, A.; Ohashi, Y.; Shiro, M.; Sasaki, K.; Shiomi, D.; Sato, K.; Takui, T.; Nakasuji, K.; Thermochromism in an organic crystal based on the coexistence of sigma- and pi-dimers. *Nat. Mater.* **2008**, 7, 48–51.

53. Molcanov, K.; Mou, Z. Y.; Kertesz, M.; Kojic-Prodic, B.; Stalke, D.; Demeshko, S.; Santic, A.; Stilinovic, V.; Pancake Bonding in pi-Stacked Trimers in a Salt of Tetrachloroquinone Anion. *Chem. -Eur. J.* **2018**, 24, 8292–8297.

54. Poduska, A.; Hoffmann, R.; Ienco, A.; Mealli, C.; "Half-Bonds" in an Unusual Coordinated S-4²⁻ Rectangle. *Chem. -Asian. J.* **2009**, 4, 302–313.

55. Zhao, L. L.; von Hopffgarten, M.; Andrada, D. M.; Frenking, G.; Energy decomposition analysis. *Wires. Comput. Mol. Sci.* **2018**, 8, e1345.

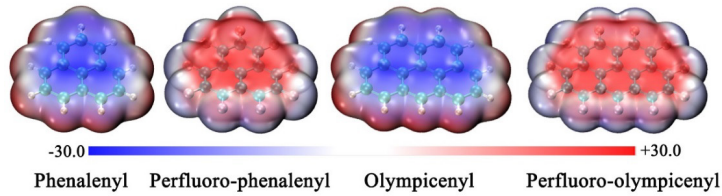
56. Zhao, L. L.; Hermann, M.; Schwarz, W. H. E.; Frenking, G.; The Lewis electron-pair bonding model: modern energy decomposition analysis. *Nat. Rev. Chem.* **2019**, 3, 48–63.

57. Andres, J.; Ayers, P. W.; Boto, R. A.; Carbo-Dorca, R.; Chermette, H.; Cioslowski, J.; Contreras-Garcia, J.; Cooper, D. L.; Frenking, G.; Gatti, C.; Heidar-Zadeh, F.; Joubert, L.; Pendas, A. M.; Matito, E.; Mayer, I.; Misquitta, A. J.; Mo, Y. R.; Pilme, J.; Popelier, P. L. A.; Rahm, M.; RamosCordoba, E.; Salvador, P.; Schwarz, W. H. E.; Shahbazian, S.; Silvi, B.; Sola, M.; Szalewicz, K.; Tognetti, V.; Weinhold, F.; Zins, E. L.; Nine questions on energy decomposition analysis. *J. Comput. Chem.* **2019**, 40, 2248–2283.

58. Vyboishchikov, S. F.; Krapp, A.; Frenking, G.; Two complementary molecular energy decomposition schemes: The Mayer and Ziegler-Rauk methods in comparison. *J. Chem.*

Phys. **2008**, *129*, 144111.

Table of Contents Graphic



Dimers of neutral polycyclic aromatic hydrocarbon (PAH) radicals display known strong electron sharing pi-stacking pancake bonding. Here we show that the cationic dimers have intermolecular pancake bonding about twice as strongly as the neutral dimers. Perfluoro substitution changes the preference and about doubles the binding energy for the anionic singly charged dimer compared to their respective the neutral ones.